

## Alkaline Phosphatase Activity of Plant Growth-Promoting Actinomycetes and Their Genetic Diversity Based on the *phoD* Gene

Muhammad Faiz Amri<sup>1</sup>, Edi Husen<sup>2</sup>, Aris Tjahjoleksono<sup>1</sup>, Aris Tri Wahyudi\*

<sup>1</sup>Department of Biology, Faculty of Mathematics and Natural Sciences, IPB University, Bogor, Indonesia

<sup>2</sup>Indonesian Soil Research Institute, Bogor, Indonesia

### ARTICLE INFO

#### Article history:

Received October 16, 2021

Received in revised form November 1, 2021

Accepted November 9, 2021

#### KEYWORDS:

alkaline phosphatase,  
genetic diversity,  
*phoD*,  
phosphate solubilization,  
protein structure modeling

### ABSTRACT

Actinomycete is one of the beneficial bacteria groups inhabiting rhizosphere soil. They can promote plant growth through various mechanisms. In the previous study we have isolated rhizosphere actinomycetes from maize rhizosphere with direct plant growth promotion characters. The aims of the present study were to analyze the ability of maize rhizosphere actinomycetes to solubilize phosphate, determine alkaline phosphatase activity, and study their genetic diversity based on *phoD* gene. Thirteen rhizosphere actinomycete isolates were able to solubilize phosphate at concentration range 55.84±2.27 mg/L to 144.48±5.71 mg/L. The activity of extracellular alkaline phosphatase was exhibited by all maize rhizosphere actinomycetes isolates in various level ranging from 0.08 mU/mL to 0.51 mU/mL. The *phoD* gene, one of the three homologous genes which encode alkaline phosphatases, was successfully detected in all isolates and identified as alkaline phosphatase D of *Streptomyces* spp. The partial *phoD* sequences of the isolates were located within metallophosphatase domain of alkaline phosphatase D. Alignment analysis showed that the deduced amino acid sequences of PhoD were mostly conserved in the isolates and *Streptomyces* spp. Essential residues involved in the active core arrangement of PhoD which binds metal ion cofactors were conserved. Constructed phylogenetic tree showed that the isolates were divided into two groups within PhoD cluster. PhoD of the isolates and *Streptomyces* spp. had closer relationship to purple acid phosphatase compared to other homologous PhoA and PhoX which form separate cluster. Generated three-dimensional structure model of partial PhoD had high similarity to alkaline phosphatase D of *Bacillus subtilis* (2YEQ) and showed overlapping structure based on super-positioning analysis.

## 1. Introduction

Actinomycetes colonize rhizosphere soil as one of the major groups in the microbial community, comprising the most significant part of the microbial population (Javed *et al.* 2020). They colonize the rhizosphere and stimulate plant growth as Plant Growth-Promoting Rhizobacteria (PGPR) by, providing nutrients and, phytohormones, alleviating stress, and suppressing pathogens. Rhizosphere actinomycetes are capable of stimulating the growth of maize and soybean sprouts. They exhibit plant growth-promoting characters, including phosphate solubilization, indole-3-acetic acid (IAA) production, and nitrogen fixation (Wahyudi *et al.* 2021; Sari

*et al.* 2021). This study highlighted the ability of rhizosphere actinomycetes to solubilize phosphate.

Phosphorus (P) is the second most essential macronutrient for plant growth and development, after nitrogen. Phosphorus is abundant in soil, but it exists mainly in insoluble forms and cannot be directly utilized by plants. Massive phosphate fertilizer input into agricultural soil is the main factor in bulking phosphate abundance. Meanwhile, plants only use a small portion of phosphate, and the rest is precipitated in soil (Soumare *et al.* 2020). Microbes are essential in the natural phosphorus cycle due to phosphate solubilization activity. They are crucial in releasing inaccessible phosphate forms in soil. Phosphate solubilization by PGPR increases its availability for plants (Kaur and Reddy 2013). Well-known mechanisms of phosphate solubilization and mineralization by PGPR are acidification

\* Corresponding Author

E-mail Address: ariswa@apps.ipb.ac.id

through organic acid production and phosphatase enzyme activity. Actinomycetes can produce various organic acids and create an acidic condition that is important for releasing bound phosphate. Two phosphatases involved in phosphate solubilization are acid phosphatase and alkaline phosphatase. Acid phosphatase is commonly found in plants, bacteria, and fungi, while alkaline phosphatase is predominantly produced by bacteria. The role of phosphatase enzymes is crucial in the enzymatic hydrolysis of soil organic P (Wan *et al.* 2020).

Alkaline phosphatase catalyzes the hydrolysis of esters and phosphoric acid anhydrides and increases the provision of soluble phosphate in soil (Khadem and Raiesi 2019). Under phosphate starvation, alkaline phosphatase activity is induced where a signal molecule binds to the promoter and activates gene expression (Shen *et al.* 2016). This enzyme is widespread in many organisms, including prokaryotes and eukaryotes, except in some higher plants (Sharma *et al.* 2014). Bacterial alkaline phosphatase synthesis is encoded by three homologous genes *phoA*, *phoX*, and *phoD*. Alkaline phosphatases produced by *phoA* and *phoX* genes are prevalent in marine bacteria, while *phoD* abundance is higher in soil bacteria, especially in Actinobacteria, Proteobacteria, and Cyanobacteria. These alkaline phosphatases have conserved active core, binding metal ions which differ in PhoA, PhoX, and PhoD, acting as catalysis cofactors (Fraser *et al.* 2015).

In the previous study, we have successfully isolated actinomycetes from the maize rhizosphere that had plant growth-promoting characteristics, such as IAA production, ability to grow in nitrogen-free medium, and ability to solubilize phosphate in agar medium *in vitro* (Wahyudi *et al.* 2019). In the present study, our objectives were to analyze the ability of actinomycetes to solubilize phosphate, determine the activity of alkaline phosphatase enzyme, and study the genetic diversity of actinomycetes based on *phoD* gene.

## 2. Materials and Methods

### 2.1. Quantitative Estimation of Phosphate Solubilization

Thirteen rhizosphere actinomycete isolates with plant growth-promoting activity isolated from maize rhizosphere (ARJ) at East Nusa Tenggara, Indonesia were used in this study (Wahyudi *et al.* 2019). Phosphate solubilized by actinomycetes was quantitatively estimated following the method described by Joshi *et al.* (2019) in triplicate with modification. One plug ( $\pm 8$  mm diameter) of 7 days old culture on solid International *Streptomyces* Project (ISP) 4 medium (composition: 10 g soluble starch, 1

g  $K_2HPO_4$ , 1 g  $MgSO_4 \cdot 7H_2O$ , 1 g NaCl, 2 g  $(NH_4)_2SO_4$ , 2 g  $CaCO_3$ , 0.001 g  $MnCl_2 \cdot 7H_2O$ , 0.001 g  $ZnSO_4 \cdot 7H_2O$ , 0.001 g  $FeSO_4 \cdot 7H_2O$ , 20 g agar, 1,000 ml distilled water) were inoculated into 50 ml of Pikovskaya broth at pH 7 and incubated with shaking at 120 rpm for 7 days at temperature 27°C. After incubation, the culture broth was centrifuged at 6,000 rpm for 30 minutes and filtered using Whatman paper No. 42 to collect cell-free supernatant. The acidity level of the medium was measured after incubation. The supernatant was mixed with a reagent composed of 10 % ascorbic acid and 0.42 % Ammonium molybdate  $\cdot 4H_2O$  in 1 N  $H_2SO_4$  (1:6). The absorbance of the solubilized phosphate was measured using a spectrophotometer at 827 nm wavelength (Sati and Pant 2018).

### 2.2. Alkaline Phosphatase Activity Assay

The alkaline phosphatase activity of actinomycetes was measured by the following the method described by Lindang *et al.* (2021) with slight modifications. One ISP 3 solid medium culture plugs were inoculated into 50 ml ISP3 broth (composition: 20 g oats, 0.001 g  $FeSO_4 \cdot 7H_2O$ , 0.001 g  $MnCl_2 \cdot 4H_2O$ , 0.001 g  $ZnSO_4 \cdot 7H_2O$ , 1,000 ml distilled water) and incubated for 60 hours (Franco-Correa *et al.* 2010; Ghorbani-Nasrabadi *et al.* 2013). After incubation, the culture was centrifuged at 6,000 rpm for 30 minutes at 4°C and filtered using Whatman paper No. 42. Cell-free supernatant was collected as crude enzyme extract. The enzyme reaction consisted of 1 ml 5 mM p-nitrophenyl phosphate (p-NPP), 1 ml 10 mM Tris Buffer, 1 ml crude enzyme extract, and 2 ml sterile distilled water. The mixture was incubated at 37°C for 1 hour. The reaction was stopped by adding 3 ml termination buffer (0,1 M NaOH and 5 mM EDTA). The absorbance of the mixture was measured using a spectrophotometer at wavelength 405 nm. A standard solution was made using p-nitrophenol (p-NP). One unit of alkaline phosphatase activity is the amount of enzyme needed to produce 1  $\mu$ mol p-NP per minute.

### 2.3. PCR Amplification of *phoD*

Genomic DNA of the actinomycetes were extracted using colony scrapping method (Brzezinska *et al.* 2013) from solid ISP 4 medium culture incubated for 7 days and isolated using Presto™ Mini gDNA Bacteria Kit (Geneaid). PCR amplification of *phoD* was performed using specific primer pair, ALPSF730: 5'-CAGTGGGACGACCACGAGGT-3' and ALPSR110: 5'-GAGGCCGATCGGCATGTCC-3' (Sakurai *et al.* 2008). PCR mix with 50  $\mu$ l total volume consist of 25  $\mu$ l MyTaq™ HS Red Mix 2x (Bioline); 5  $\mu$ l forward primer (10 pmol); 5  $\mu$ l reverse primer (10 pmol); 5  $\mu$ l DNA template ( $\pm 100$  ng/L); and 10  $\mu$ l nuclease-

free water. The targeted DNA fragment was  $\pm 371$  bp. PCR was performed in condition: initial denaturation at 94°C for 3 minutes, 35 cycles of denaturation at 94°C for 1 minute, annealing at 57°C for 1 minute, extension at 72°C for 2 minutes, and final extension at 72°C for 5 minutes. Amplicons were run using 1% agarose gel electrophoresis and visualized by UV-transilluminator. Confirmed amplicons as a specific band were sequenced in FirstBase Malaysia.

#### 2.4. Amino Acid Sequences Alignment and Phylogenetic Tree Construction

The obtained nucleotide sequences were analyzed and edited using BioEdit program and identified using BlastX program on National Centre for Biotechnology Information (NCBI) website (<https://blast.ncbi.nlm.nih.gov/Blast.cgi>). Nucleotide sequences of *phoD* were deduced into amino acids on ExPasy website (<https://web.expasy.org/translate/>) and aligned in BioEdit program using ClustalW method. Reference sequences used in this analysis were Alkaline phosphatase D *Bacillus subtilis* (2YEQ), Alkaline phosphatase [*Streptomyces cellulosa*] (GHE70673.1), Alkaline phosphatase D family protein [*Streptomyces* sp.] S10(2018) (WP\_127896412.1), MULTISPECIES: Alkaline phosphatase D family protein [*Streptomyces*] (WP\_161378451.1), MULTISPECIES: Alkaline phosphatase D family protein [*Streptomyces*] (WP\_037761763.1), Alkaline phosphatase D family protein [*Streptomyces* sp. H23] (WP\_134654220.1), Alkaline phosphatase D family protein [*Streptomyces tendae*] (WP\_189744243.1), and Alkaline phosphatase D family protein [*Streptomyces tendae*] (WP\_159324759.1). Alkaline phosphatase D of *Bacillus subtilis* (2YEQ) was used for functional residues comparison. Phylogenetic tree of the actinomycetes was constructed in MEGA.X program using neighbor-joining method with 1000x bootstrap.

#### 2.5. Domain Prediction and Three-dimensional Structure Modeling

Actinomycete with the highest alkaline phosphatase activity was used for domain prediction and three-dimensional protein structure modeling. Domain prediction of partial PhoD of the actinomycete and its relative position within complete *Streptomyces* alkaline phosphatase D was performed in InterPro classification of protein (<https://www.ebi.ac.uk/interpro/>) (Hunter *et al.* 2009). MULTISPECIES: Alkaline phosphatase D family protein [*Streptomyces*] (WP\_161378451.1) was used for reference. Three-dimensional protein structure model was constructed on I-TASSER website (<https://zhanggroup.org/I-TASSER/>) (Zhang 2008). The I-TASSER program was used to construct structure model of the query

protein (PhoD) based on the highest matching with known protein structure in the Protein Data Bank (PDB) Library and assess the biological function and topological similarities with native protein (Yang and Zhang 2015). The constructed three-dimensional model visualization and super-positioning analysis were performed using UCSF ChimeraX (Pettersen *et al.* 2021) to observe the overlapping region and the position of essential residues with *Bacillus subtilis* PhoD as reference.

### 3. Results

#### 3.1. Phosphate Solubilization and Alkaline Phosphatase Activity

All isolates solubilized tricalcium phosphate in Pikovskaya broth at a varied concentration of 55.84 $\pm$ 2.27 mg/L to 144.55 $\pm$ 5.71 mg/L (Figure 1). Actinomycete isolate with the highest phosphate solubilization activity was ARJ 38, while the lowest was ARJ 32. Total inorganic phosphate solubilized by all isolates were higher than *Bradyrhizobium japonicum* BJ11, except ARJ 32. The medium acidity after incubation period generally decreased from initial pH 7 to 5. All isolates exhibited alkaline phosphatase activity in various level range from 0.08 mU/ml (ARJ 13) to 0.51 mU/ml (ARJ 47) (Figure 2). These activities were comparable to *B. japonicum* BJ11.

#### 3.2. PCR Amplification and Amino Acid Sequence Alignment

The *phoD* gene was detected in all isolates as a specific band of  $\pm 371$  bp amplicons based on UV visualization (Figure 3). Partial sequences of isolates *phoD* gene were homologous to alkaline phosphatase D from *Streptomyces* with 96 to 100% similarity and 98 to 100% query cover (Table 1).

Partial nucleotide sequences of the isolates were deduced into amino acids consisted of 118 residues. Amino acid sequences of isolates PhoD were aligned with PhoD reference sequences of *Streptomyces* spp. and *Bacillus subtilis* (2YEQ) (Figure 4). Eighty percent of total residues were highly conserved in *Streptomyces* spp. Domain prediction of complete *Streptomyces* spp. PhoD and relative position of the deduced amino acid position was displayed in Figure 5. The predicted domains were TAT signal, N-terminal, and metallophosphatase. The partial amino acid sequence of the isolates was part of metallophosphatase domain in PhoD-like phosphatase (IPR018946), a member of metallophosphatase (MPP) superfamily. Essential residues double aspartic acid and double asparagine, which binds Ca<sup>2+</sup> in the active site, were observed in the corresponding position of Asp<sup>209</sup>, Asp<sup>210</sup>, Asn<sup>215</sup>, Asn<sup>216</sup> of *B. subtilis* PhoD (2YEQ).

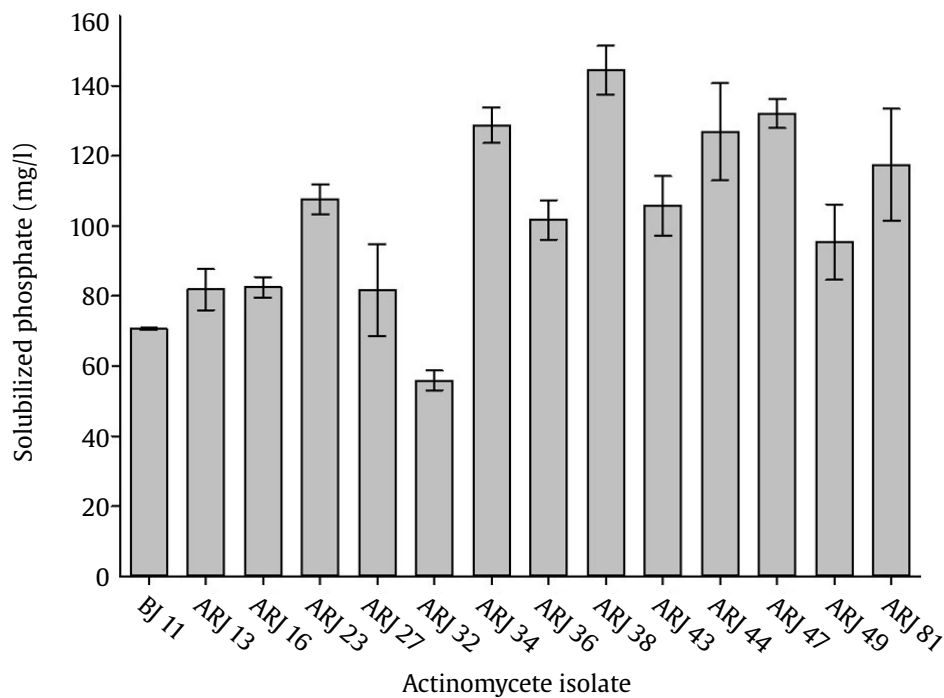


Figure 1. The concentration of phosphate solubilized by rhizosphere actinomycetes isolates. BJ11: *Bradyrhizobium japonicum* BJ11

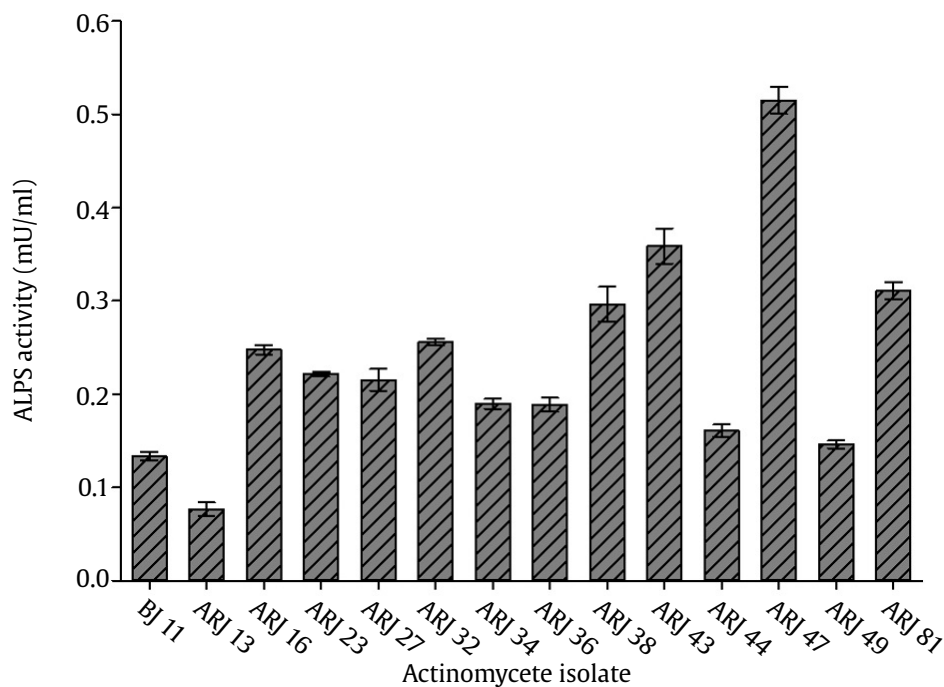


Figure 2. Alkaline phosphatase activity of rhizosphere actinomycetes isolates. ALPS: alkaline phosphatase, BJ11: *Bradyrhizobium japonicum* BJ11.

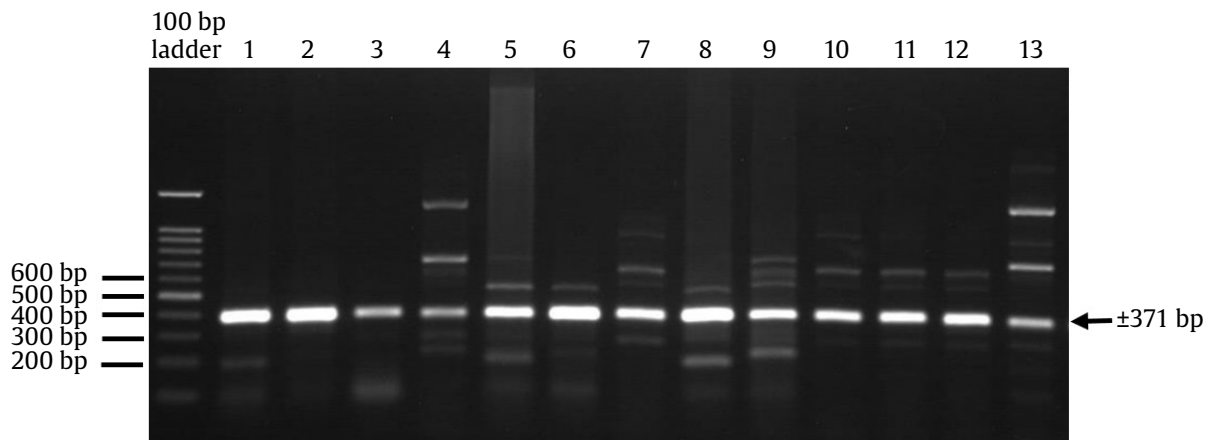


Figure 3. Visualization of the amplified *phoD* gene. 1. ARJ 13, 2. ARJ 16, 3. ARJ 23, 4. ARJ 27, 5. ARJ 32, 6. ARJ 34, 7. ARJ 36, 8. ARJ 38, 9. ARJ 43, 10. ARJ 44, 11. ARJ 47, 12. ARJ 49, 13. ARJ 81

Table 1. Identity of *phoD* gene of maize rhizosphere actinomycetes

Actinomycete	Homologous sequence	Query cover (%)	Similarity (%)	E-value	Accession number
ARJ 13	alkaline phosphatase D family protein [ <i>Streptomyces</i> sp. S10(2018)]	98	97	1e-72	WP_127896412.1
ARJ 16	alkaline phosphatase [ <i>Streptomyces cellulosa</i> ]	98	97	2e-73	GHE70673.1
ARJ 23	alkaline phosphatase D family protein [ <i>Streptomyces</i> sp. S10(2018)]	99	98	5e-72	WP_127896412.1
ARJ 27	alkaline phosphatase [ <i>Streptomyces cellulosa</i> ]	99	98	5e-74	GHE70673.1
ARJ 32	alkaline phosphatase D family protein [ <i>Streptomyces</i> sp. S10(2018)]	100	98	2e-73	WP_127896412.1
ARJ 34	MULTISPECIES: alkaline phosphatase D family protein [ <i>Streptomyces</i> ]	99	100	7e-81	WP_037761763.1
ARJ 36	alkaline phosphatase D family protein [ <i>Streptomyces</i> sp. S10(2018)]	99	98	7e-74	WP_127896412.1
ARJ 38	MULTISPECIES: alkaline phosphatase D family protein [ <i>Streptomyces</i> ]	98	97	2e-73	WP_161378451.1
ARJ 43	MULTISPECIES: alkaline phosphatase D family protein [ <i>Streptomyces</i> ]	99	97	8e-72	WP_161378451.1
ARJ 44	MULTISPECIES: alkaline phosphatase D family protein [ <i>Streptomyces</i> ]	98	97	4e-73	WP_161378451.1
ARJ 47	alkaline phosphatase D family protein [ <i>Streptomyces</i> sp. S10(2018)]	99	96	6e-71	WP_127896412.1
ARJ 49	alkaline phosphatase [ <i>Streptomyces cellulosa</i> ]	99	98	5e-74	GHE70673.1
ARJ 81	MULTISPECIES: alkaline phosphatase D family protein [ <i>Streptomyces</i> ]	100	97	1e-73	WP_161378451.1

In some isolates, there were mutations of Asp<sup>3</sup> to Glu<sup>3</sup> and Asn<sup>10</sup> to Lys<sup>10</sup>.

### 3.3. Phylogenetic Tree Analysis

Phylogenetic tree of PhoD was constructed based on deduced amino acid sequences of the isolates, *Streptomyces* spp., homologous PhoA and PhoX, and Purple Acid Phosphatase. Two distinct clusters were observed; cluster 1 members were all alkaline

phosphatase D and purple acid phosphatase of sweet potato, while cluster 2 includes PhoX and PhoA (Figure 6). The isolates were consistently included in cluster 1 and showed closer relation to PhoD of *B. subtilis* than purple acid phosphatase. They were separated into smaller groups; group 1 consisted of ARJ 13, ARJ 23, ARJ 32, ARJ 36, ARJ 38, ARJ 43, ARJ 44, ARJ 47, ARJ 81, and group 2 consisted of ARJ 16, ARJ 27, ARJ 49. PhoX and PhoA formed their cluster separated from PhoD.

2YEQ	207	TWDDHEVE <span style="color:red">NN</span> YAN--KIPEKQ--SVEAFVLRRAAYQAYYEHMPLRISLPLNGPDMQLYRHF	265
ARJ_13	1	QW <span style="color:red">ED</span> QEV <span style="color:red">NN</span> WYPGQVVADTDDRYTEKSVDVLAARARRAFSEYFP <span style="background-color:lightgrey">IST</span> -LRPGAREGRVHRVL	62
ARJ_23	1	QW <span style="color:red">DD</span> QEV <span style="color:red">NN</span> WYPGQVVADTDDRYTEKSVDVLAARARRAFSEYFP <span style="background-color:lightgrey">IST</span> -LRPGAREGRVHRVL	62
ARJ_32	1	QW <span style="color:red">DD</span> PEVR <span style="color:red">NK</span> WYPGQVVADTDDRYTEKSVDVLAARARRAFSEYFP <span style="background-color:lightgrey">IST</span> -LRPGAREGRVHRVL	62
ARJ_34	1	QW <span style="color:red">DD</span> HEVR <span style="color:red">NN</span> WYPGQVIADTDDRYTEKSVDVLAGRARRAFSEYFP <span style="background-color:lightgrey">IST</span> -LRPGAREGRVHRVL	62
ARJ_36	1	QW <span style="color:red">ED</span> QEV <span style="color:red">NN</span> WYPGQVVADTDDRYTEKSVDVLAARARRAFSEYFP <span style="background-color:lightgrey">IST</span> -LRPGAREGRVHRVL	62
ARJ_38	1	QW <span style="color:red">ED</span> QKVR <span style="color:red">NN</span> WYPGQVVADTDDRYTEKSVDVLAARARRAFSEYFP <span style="background-color:lightgrey">IST</span> -LRPGAREGRVHRVL	62
ARJ_43	1	QW <span style="color:red">ED</span> QEF <span style="color:red">GN</span> WYPGQVVADTDDRYTEKSVDVLAARARRAFSEYFP <span style="background-color:lightgrey">IST</span> -LRPGAREGRVHRVL	62
ARJ_44	1	QW <span style="color:red">ED</span> QEV <span style="color:red">NK</span> WYPGQVVADTDDRYTEKSVDVLAARARRAFSEYFP <span style="background-color:lightgrey">IST</span> -LRPGAREGRVHRVL	62
ARJ_47	1	QW <span style="color:red">ED</span> QEV <span style="color:red">GN</span> WYPGQVVADTDDRYTEKSVDVLAARARRAFSEYFP <span style="background-color:lightgrey">IST</span> -LRPGAREGRVHRVL	62
ARJ_81	1	QW <span style="color:red">ED</span> QEV <span style="color:red">NK</span> WYPGQVVADTDDRYTEKSVDVLAARARRAFSEYFP <span style="background-color:lightgrey">IST</span> -LRPGAREGRVHRVL	62
ARJ_16	1	QW <span style="color:red">DD</span> HEVR <span style="color:red">NN</span> WYPGQRIADTTRYTMKDVDVLAARARRAFGEYYPVST-LRPGAREGRVHRVL	62
ARJ_27	1	QW <span style="color:red">DD</span> HEVR <span style="color:red">NN</span> WYPGQRIADTTRYTVKDVLDVLAARARRAFGEYYPVST-LRPGAREGRVHRVL	62
ARJ_49	1	QW <span style="color:red">DD</span> HEVR <span style="color:red">NN</span> WYPGQRIADTTRYTVKDVLDVLAARARRAFGEYYPVST-LRPGAREGRVHRVL	62
GHE70673.1	248	QW <span style="color:red">DD</span> HEVR <span style="color:red">NN</span> WYPGQRIADTTRYTVKDVLDVLAARARRAFGEYYPVST-LRPGAREGRVHRVL	309
WP_127896412.1	249	QW <span style="color:red">DD</span> HEVR <span style="color:red">NN</span> WYPGQVVADTDDRYTEKSVDVLAARARRAFSEYFP <span style="background-color:lightgrey">IST</span> -LRPGAREGRVHRVL	310
WP_161378451.1	249	QW <span style="color:red">DD</span> HEVR <span style="color:red">NN</span> WYPGQVVADTDDRYTEKSVDVLAARARRAFSEYFP <span style="background-color:lightgrey">IST</span> -LRPGAREGRVHRVL	310
WP_037761763.1	249	QW <span style="color:red">DD</span> HEVR <span style="color:red">NN</span> WYPGQVIADTDDRYTEKSVDVLAGRARRAFSEYFP <span style="background-color:lightgrey">IST</span> -LRPGAREGRVHRVL	310
WP_134654220.1	249	QW <span style="color:red">DD</span> HEVR <span style="color:red">NN</span> WYPGQVIADTDDRYTEKSVDVLAARARRAFGEYFP <span style="background-color:lightgrey">IST</span> -LRPGAREGRVHRVL	310
WP_189744243.1	249	QW <span style="color:red">DD</span> HEVR <span style="color:red">NN</span> WYPGQVVADTDDRYTEKSVDVLAARARRAFSEYFP <span style="background-color:lightgrey">IST</span> -LRPGAREGRVHRVL	310
WP_159324759.1	249	QW <span style="color:red">DD</span> HEVR <span style="color:red">NN</span> WYPGQVVADTDDRYTEKSVDVLAARARRAFSEYFP <span style="background-color:lightgrey">IST</span> -LRPGAREGRVHRVL	310
2YEQ	266	TYGNLASFNVLDTROYRDDQANN <span style="background-color:lightgrey">DGNKPP</span> SD <span style="background-color:lightgrey">ESRN</span> PNRTLLGKEQEQWLFNNLGSSTAHNVL <span style="background-color:lightgrey">A</span>	329
ARJ_13	63	RQG <span style="background-color:lightgrey">PLLDVFLDMR</span> TYRNANS-----PGGQTVDF-QGILGREQLEWLKRELARSRAVWKVIA	118
ARJ_23	63	RQG <span style="background-color:lightgrey">PLLDVFLDMR</span> TYRNANS-----PGGQTVDF-QGILGREQLEWLKRELARSRAVWKVIA	118
ARJ_32	63	RQG <span style="background-color:lightgrey">PLLDVFLDMR</span> TYRNANS-----PGGQTVDF-QGILGREQLEWLKRELARSRAVWKVIA	118
ARJ_34	63	RQG <span style="background-color:lightgrey">PLLDVFLDMR</span> TYRNANS-----PGGQSEDF-QGILGREQLEWLKRELARSRAVWKVIA	118
ARJ_36	63	RQG <span style="background-color:lightgrey">PLLDVFLDMR</span> TYRNANS-----PGGQTVDF-QGILGREQLEWLKRELARSRAVWKVIA	118
ARJ_38	63	RQG <span style="background-color:lightgrey">PLLDVFLDMR</span> TYRNANS-----PGGQTVDF-QGILGREQLEWLKRELARSRAVWKVIA	118
ARJ_43	63	RQG <span style="background-color:lightgrey">PLLDVFLDMR</span> TYRNANS-----PGGQTVDF-QGILGREQLEWLKRELARSRAVWKVIA	118
ARJ_44	63	RQG <span style="background-color:lightgrey">PLLDVFLDMR</span> TYRNANS-----PGGQTVDF-QGILGREQLEWLKRELARSRAVWKVIA	118
ARJ_47	63	RQG <span style="background-color:lightgrey">PLLDVFLDMR</span> TYRNANS-----PGGQTVDF-QGILGREQLEWLKRELARSRAVWKVIA	118
ARJ_81	63	RQG <span style="background-color:lightgrey">PLLDVFLDMR</span> TYRNANS-----PGGQTVDF-QGILGREQLEWLKRELARSRAVWKVIA	118
ARJ_16	63	RQG <span style="background-color:lightgrey">PLLDVFLDMR</span> TYRNANS-----PGDRTVDF-QGILGREQLDWLKRELTRSAVW----	115
ARJ_27	63	RQG <span style="background-color:lightgrey">PLLDVFLDMR</span> TYRNANS-----PGDRTVDF-QGILGREQLDWLKRELTRSAVWKVIA	118
ARJ_49	63	RQG <span style="background-color:lightgrey">PLLDVFLDMR</span> TYRNANS-----PGDRTVDF-QGILGREQLDWLKRELTRSAVWKVIA	118
GHE70673.1	310	RQG <span style="background-color:lightgrey">PLLDVFLDMR</span> TYRNANS-----PSDRTVDF-QGILGREQLDWLKRELTRSAVWKVIA	365
WP_127896412.1	311	RQG <span style="background-color:lightgrey">PLLDVFLDMR</span> TYRNANS-----PGGQTVDF-QGILGREQLEWLKRELARSRAVWKVIA	366
WP_161378451.1	311	RQG <span style="background-color:lightgrey">PLLDVFLDMR</span> TYRNANS-----PGGQTVDF-QGILGREQLEWLKRELARSRAVWKVIA	366
WP_037761763.1	311	RQG <span style="background-color:lightgrey">PLLDVFLDMR</span> TYRNANS-----PGGQSEDF-QGILGREQLEWLKRELARSRAVWKVIA	366
WP_134654220.1	311	RQG <span style="background-color:lightgrey">PLLDVFLDMR</span> TYRNANS-----PGGQTVDF-QGILGREQLEWLKRELARSRAVWKVIA	366
WP_189744243.1	311	RQG <span style="background-color:lightgrey">PLLDVFLDMR</span> TYRNANS-----PGEQTVDF-QGILGREQLEWLKRELARSRAVWKVIA	366
WP_159324759.1	311	RQG <span style="background-color:lightgrey">PLLDVFLDMR</span> TYRNANS-----PGQQTVDF-QGILGREQLEWLKRELARSRAVWKVIA	366

Figure 4. Deduced amino acid alignment of partial phoD of rhizosphere actinomycete isolates, *Bacillus subtilis*, and *Streptomyces* spp. Red: conserved residues involved in the active site of PhoD. Light grey color: conserved residues of the isolates and *Streptomyces* spp. Dark grey: conserved residues of the isolates, *B. subtilis*, and *Streptomyces* spp.

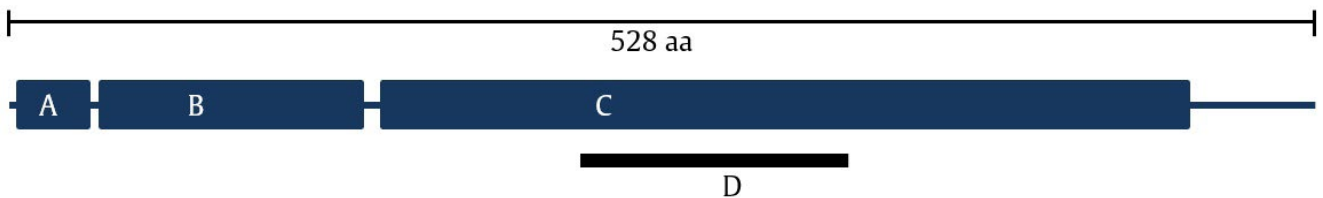


Figure 5. Domain prediction of complete *Streptomyces* PhoD (528 residues) (WP\_161378451.1) and deduced amino acid position of ARJ 47. A. TAT signal (IPR006311), B. PhoD N-terminal (IPR032093), C. Metallophosphatase domain (IPR018946), D. ARJ 47 partial PhoD (118 residues)

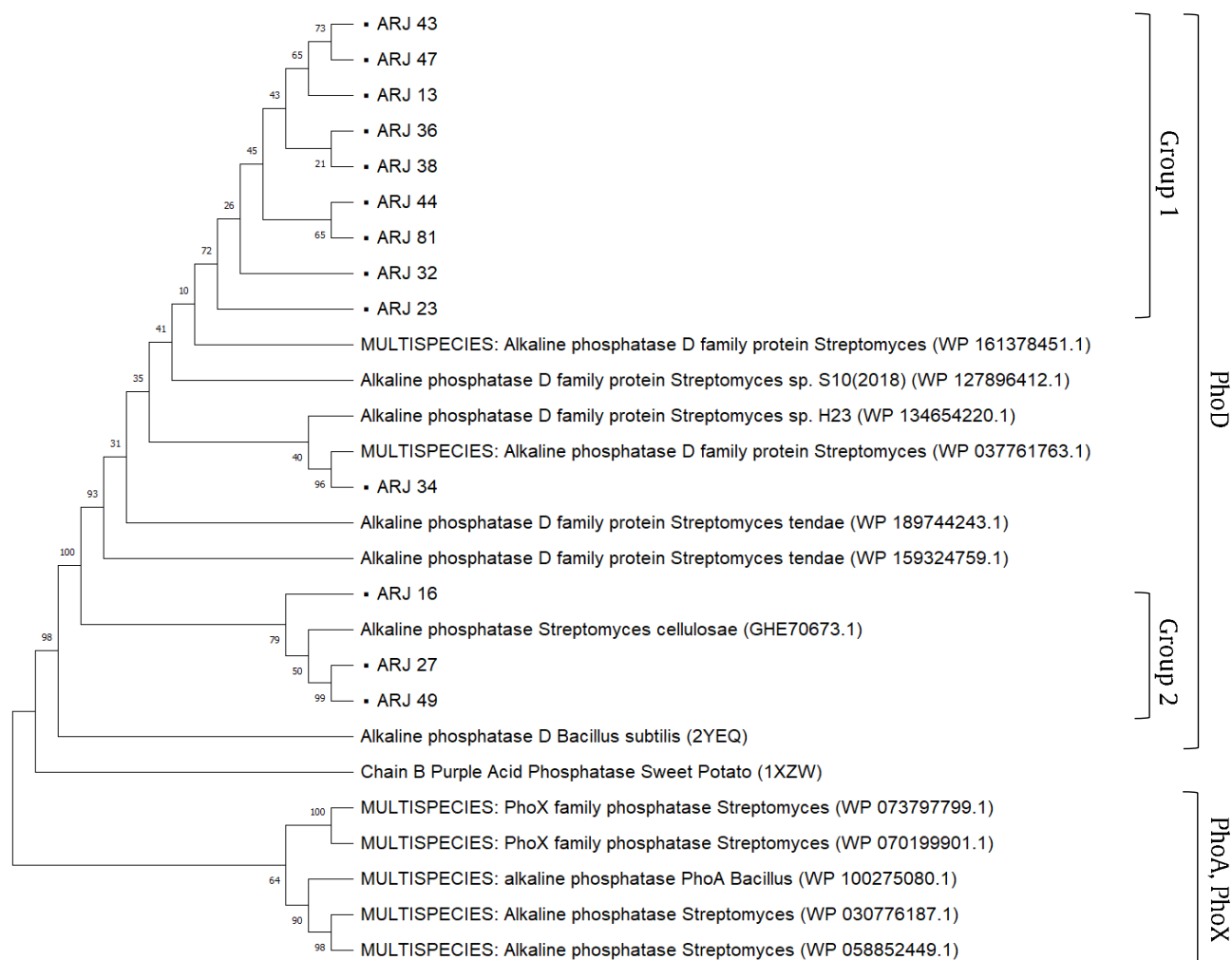


Figure 6. Constructed phylogenetic tree based on partial PhoD amino acid sequences

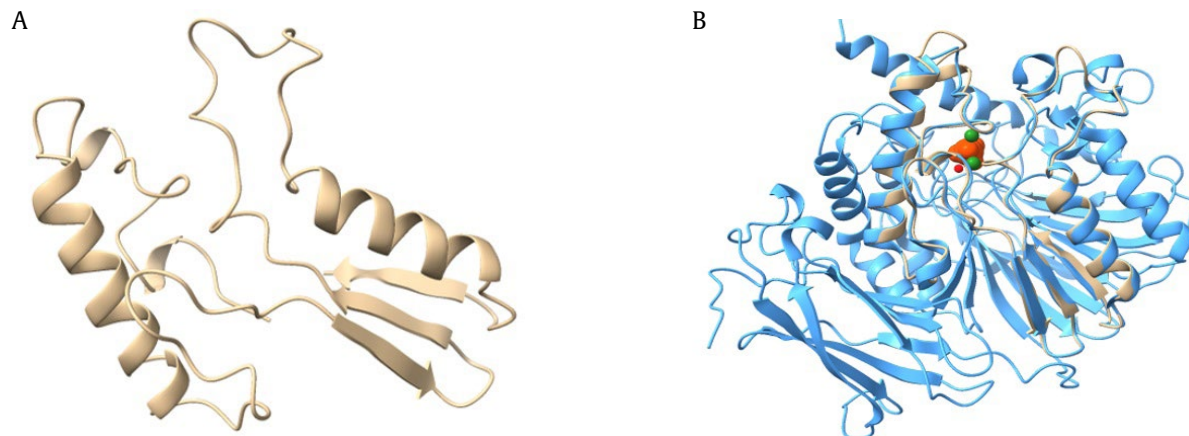


Figure 7. 3D structure prediction and superposition to PhoD *B. subtilis* (2YEQ). A. Partial PhoD of ARJ 47. B. Superposition of partial PhoD ARJ 47 (cream) and PhoD *B. subtilis* (2YEQ) (light blue), Phosphate (orange),  $\text{Ca}^{2+}$  (green),  $\text{Fe}^{3+}$  (red)

### 3.4. 3D Structure Model Prediction and Superposition Analysis

A three-dimensional structure model of partial PhoD generated by I-TASSER is displayed in Figure 7. The quality of this model was described by several parameters, including C-score, TM-score, and RMSD. Predicted model of PhoD had C-score 0,44, TM-score  $0.77\pm 0.1$  and RMSD  $3.4\pm 2.4\text{Å}$ . These values indicated high topological structure similarity with native proteins. The PhoD model had analogy with PhoD of *B. subtilis* (2YEQ) with TM-score 0.939 and RMSD 0.89 Å. These results indicated that the models could be trusted. Super-positioning analysis showed similar structure to a particular region of 2YEQ.

## 4. Discussion

Rhizosphere actinomycete isolates exhibited phosphate solubilization and alkaline phosphatase activity. All isolates solubilized phosphate in various concentration. ARJ 38 was quantitatively estimated to solubilize phosphate at the highest concentration, while ARJ 32 was the lowest. The ability of isolates to solubilize phosphate was lower compared to *Streptomyces* sp. WA-1 and *S. djakartensis* TB-4, which solubilize phosphate up to 721.3 mg/L and 703.6 mg/L, respectively (Anwar *et al.* 2016). The result was higher than *P. aeruginosa* DRB1, with solubilization activity observed at 33.7 mg/L (Wong *et al.* 2021). Generally, the acidity of the medium after incubation period decreased from pH 7 to 5. The negative correlation between the amount of solubilized phosphate and the decrease of medium acidity after incubation was quite unclear. This indicates the possibility of phosphate solubilization mechanism by organic acid production. *Streptomyces* sp. mhcr0816 and *Streptomyces* sp. mhce0811 mainly produced malate and gluconate, respectively, and resulted in phosphate solubilization up to 1916.12 mg/L (Jog *et al.* 2014). The decreases of initial medium acidity may indicate microbial phosphate solubilization by acid production and phosphatase enzyme activity (Rubio *et al.* 2015).

Alkaline phosphatase catalyzes the hydrolysis of p-NPP into p-NP and inorganic orthophosphate leads to yellow color formation in a buffered solution in alkaline conditions (Chen *et al.* 2018). The activity of alkaline phosphatase is affected by acidity. The increase in alkaline phosphatase activity was reported from pH 5 and reached optimal at pH 9 (Behera *et al.* 2017). This enzyme is essential in soil microbial

phosphate solubilization, where soil acidity is mainly neutral and favorable for its activity. Extracellular alkaline phosphatase activity exhibited by all isolates was comparable to other soil actinomycetes isolates with 0.59–27.59 mU/ml (Ghorbani-Nasrabadi *et al.* 2013). Intracellular alkaline phosphatase activity of actinomycetes isolated from *Trifolium repens* L. was recorded at higher level 10-15 U (Franco-Correa *et al.* 2010). Actinomycetes alkaline phosphatase activity is relatively lower than non-actinomycetes bacteria (Lindang *et al.* 2021). However, the highest abundance of soil microbial alkaline phosphatase was found in actinomycetes. A recent study reported that not all *phoD* harboring soil bacteria contributed to the secretion of ALPS involved in soil phosphate solubilization (Zhu *et al.* 2021).

The presence of *phoD* in all isolates confirmed their ability to produce alkaline phosphatase involved in phosphate solubilization. The amino acid alignment showed that most residues of partial PhoD were highly conserved in *Streptomyces*. They had high variation compared to *B. subtilis* PhoD (2YEQ). However, essential residues involved in binding two  $\text{Ca}^{2+}$  ions were conserved even though mutations occurred in some isolates. These mutations did not affect the activity level of ALPS. Complete sequence *Streptomyces* PhoD consisted of 3 domains: twin-arginine translocation (TAT) signal, N-terminal, and metallophosphatase. Tat signal is involved in PhoD transport via Tat-dependent pathway, which is conserved in several bacteria. Partial PhoD of the isolates and the active site is within metallophosphatase domain. The diversity of *phoD* in soil microorganisms has been recorded through metagenomic approach. Actinomycetales order was the most abundant *phoD* possessing bacteria group in grassland soil (Ragot *et al.* 2015). In another study, the abundance *phoD* of actinobacteria was higher than other bacteria groups in swine manure-treated soil (Chen *et al.* 2019). Soil conditions may affect the abundance of *phoD*. Microbial community in soil under organic matter amendment showed an increase of alkaline phosphatase, where *phoD* is involved, as a response to low P availability (Fraser *et al.* 2015). On the other hand, the community structure of *phoD* harboring bacteria was relatively stable in soil with different P amendment levels, mainly dominated by Actinobacteria, Cyanobacteria, and Proteobacteria (Ragot *et al.* 2015). To date, there is still no clear description of actinomycetes *phoD*.

PhoA, PhoX, and PhoD are homologous alkaline phosphatases synthesized during phosphate deficiency in bacteria. These enzymes are members of metallophosphatase superfamily, which is characterized by metal ions bound in the active site. PhoA is a homodimeric phosphomonoesterase with metal ions  $Mg^{2+}$  and  $Zn^{2+}$  as cofactors (Rodriguez *et al.* 2014). PhoX and PhoD are monomeric enzymes. PhoX is solely phosphomonoesterases and has two  $Fe^{3+}$  and three  $Ca^{2+}$  ions as cofactors. PhoD is mainly phosphodiesterases but capable of hydrolyzing phosphomonoesters. The cofactor of this enzyme are one  $Fe^{3+}$  and two  $Ca^{2+}$ . Within metallophosphatase superfamily, PhoD diverged from PhoA and PhoX families, forming an exclusive subgroup. PhoD has the closest relation to purple acid phosphatase. In this enzyme, two  $Ca^{2+}$  ions are replaced by one metal ion of either  $Fe^{2+}$ ,  $Mn^{2+}$ , or  $Zn^{2+}$  (Rodriguez *et al.* 2014). This information was consistently displayed by the constructed phylogenetic tree of partial PhoD. PhoA and PhoX formed their group separated from PhoD, which had a closer relationship with purple acid phosphatase.

Generated three-dimensional structure model of partial PhoD was assumed correct and trustworthy, indicated by the high value of model quality parameters. C-score (confidence score) represents the overall accuracy of the predicted protein structure with a value range of -5 to 2, a higher value indicates better quality of protein model. Protein with C-score more than -1.5 is expected to have correct folding. TM-score and RMSD are widely used to estimate topological structure similarity between predicted model and native protein. TM-score value ranges from 0 to 1, a higher value indicates higher structural match (Saepuloh *et al.* 2020). The analogy with *B. subtilis* PhoD (2YEQ) showed their similarity as most ARJ 47 partial PhoD structures were overlapping. Four residues involved in binding two  $Ca^{2+}$  ions that directly interact with phosphate substrate occupied the correct position. It was predicted that the two  $Ca^{2+}$  ions were also present in the active core of *Streptomyces* PhoD.

In conclusion, actinomycetes isolated from maize rhizosphere exhibited phosphate solubilization and alkaline phosphatase activity, confirmed by the presence of *phoD* gene which identified as alkaline phosphatase D of *Streptomyces* spp. Deduced amino acid alignment revealed that most of its residues were highly conserved in *Streptomyces* spp. Essential residues which bind  $Ca^{2+}$  cofactors in the active site of the enzyme were detected. PhoD had closer relationship to purple acid phosphatase than the homologous PhoA and PhoX. Partial PhoD was located within metallophosphatase domain of metallophosphatase superfamily. Three-dimensional structure model of

partial PhoD had high topological similarity to *Bacillus subtilis* PhoD and showed overlapping structure. This study revealed the first information regarding genetic diversity of rhizosphere actinomycetes partial PhoD and its predicted three-dimensional structure. Further attempt to provide complete structure of rhizosphere actinomycetes PhoD is interesting to be done since there are still no registered information in the protein data bank.

## Acknowledgements

This work was financially supported by University Excellence-Basic Research (“Penelitian Dasar-Unggulan Perguruan Tinggi”/PD-UPT) from The Ministry of Research and Technology /National Research and Innovation Agency of the Republic of Indonesia 2021 [1/E1/KP.PTNBH/2021] to ATW. The authors thank for all the support to carry out this research.

## References

- Anwar, S., Ali, B., Sajid, I., 2016. Screening of rhizospheric actinomycetes for various *in-vitro* and *in-vivo* plant growth promoting (PGP) traits and for agroactive compounds. *Front Microbiol.* 7, 1334. <https://doi.org/10.3389/fmicb.2016.01334>
- Behera, B.C., Yadav, H., Singh, S.K., Sethi, B.K., Mishra, R.R., Kumari, S., Thatoi, H., 2017. Alkaline phosphatase activity of a phosphate solubilizing *Alcaligenes faecalis*, isolated from mangrove soil. *Biotechnol. Res. Innov.* 1, 101-111. <https://doi.org/10.1016/j.biori.2017.01.003>
- Brzezinska, M.S., Jankiewicz, U., Walczak, M., 2013. Biodegradation of chitinous substances and chitinase production by the soil actinomycete *Streptomyces rimosus*. *Int. Biodeterior. Biodegrad.* 84, 104-110. <https://doi.org/10.1016/j.ibiod.2012.05.038>
- Chen, C., Zhao, J., Lu, Y., Sun, J., Yang, X., 2018. Fluorescence immunoassay based on the phosphate-triggered fluorescence turn-on detection of alkaline phosphatase. *Anal. Chem.* 90, 3505-3511. <https://doi.org/10.1021/acs.analchem.7b05325>
- Chen, X., Jiang, N., Condrón, L.M., Dunfield, K.E., Chen, Z., Wang, J., Chen, L., 2019. Soil alkaline phosphatase activity and bacterial *phoD* gene abundance and diversity under long-term nitrogen and manure inputs. *Geoderma.* 349, 36-44. <https://doi.org/10.1016/j.geoderma.2019.04.039>
- Franco-Correa, M., Quintana, A., Duque, C., Suarez, C., Rodríguez, M.X., Barea, J.M., 2010. Evaluation of actinomycete strains for key traits related with plant growth promotion and mycorrhiza helping activities. *Appl. Soil. Ecol.* 45, 209-217. <https://doi.org/10.1016/j.apsoil.2010.04.007>
- Fraser, T., Lynch, D.H., Entz, M.H., Dunfield, K.E., 2015. Linking alkaline phosphatase activity with bacterial *phoD* gene abundance in soil from a long-term management trial. *Geoderma.* 257, 115-122. <https://doi.org/10.1016/j.geoderma.2014.10.016>
- Ghorbani-Nasrabadi, R., Greiner, R., Alikhani, H.A., Hamed, J., Yakhchali, B., 2013. Distribution of actinomycetes in different soil ecosystems and effect of media composition on extracellular phosphatase activity. *J. Soil. Sci. Plant. Nutr.* 13, 223-236. <https://doi.org/10.4067/S0718-95162013005000020>

- Hunter, S., Apweiler, R., Attwood, T.K., Bairoch, A., Bateman, A., Binns, D., Bork, P., Das, U., Daugherty, L., Duquenne, L., Finn, R.D., 2009. InterPro: the integrative protein signature database. *Nucleic Acids Res.* 37, 211-215. <https://doi.org/10.1093/nar/gkn785>
- Javed, Z., Tripathi, G.D., Mishra, M., Dashora, K., 2020. Actinomycetes–The microbial machinery for the organic-cycling, plant growth, and sustainable soil health. *Biocatal. Agric. Biotechnol.* 31, 101893. <https://doi.org/10.1016/j.bcab.2020.101893>
- Jog, R., Pandya, M., Nareshkumar, G., Rajkumar, S., 2014. Mechanism of phosphate solubilization and antifungal activity of *Streptomyces* spp. isolated from wheat roots and rhizosphere and their application in improving plant growth. *Microbiology.* 160, 778-788. <https://doi.org/10.1099/mic.0.074146-0>
- Joshi, E., Iyer, B., Rajkumar, S., 2019. Glucose and arabinose dependent mineral phosphate solubilization and its succinate-mediated catabolite repression in *Rhizobium* sp. RM and RS. *J. Biosci. Bioeng.* 28, 551-557. <https://doi.org/10.1016/j.jbiosc.2019.04.020>
- Kaur, G., Reddy, M.S., 2013. Role of phosphate-solubilizing bacteria in improving the soil fertility and crop productivity in organic farming. *Arch. Agron. Soil. Sci.* 60, 549-564. <https://doi.org/10.1080/03650340.2013.817667>
- Khadem, A., Raiesi, F., 2019. Response of soil alkaline phosphatase to biochar amendments: changes in kinetic and thermodynamic characteristics. *Geoderma.* 337, 44-54. <https://doi.org/10.1016/j.geoderma.2018.09.001>
- Lindang, H.U., Subbiah, V.K., Rodrigues, K.F., Budiman, C., 2021. Isolation, identification, and characterization of phosphate solubilizing bacteria, *Paenibacillus* sp., from the soil of Danum Valley Tropical Rainforest, Sabah, Malaysia. *Biodiversitas.* 22, 4370-4378. <https://doi.org/10.13057/biodiv/d221030>
- Pettersen, E.F., Goddard, T.D., Huang, C.C., Meng, E.C., Couch, G.S., Croll, T.I., Morris, J.H., Ferrin, T.E., 2021. UCSF ChimeraX: structure visualization for researchers, educators, and developers. *Protein. Sci.* 30, 70-82. DOI:10.1002/pro.3943
- Ragot, S.A., Kertesz, M.A., Bünemann, E.K., 2015. *phoD* alkaline phosphatase gene diversity in soil. *Appl. Environ. Microbiol.* 81, 7281-7289. <https://doi.org/10.1128/AEM.01823-15>
- Rodriguez, F., Lillington, J., Johnson, S., Timmel, C.R., Lea, S.M., Berks, B.C., 2014. Crystal structure of the *Bacillus subtilis* phosphodiesterase PhoD reveals an iron and calcium-containing active site. *J. Biol. Chem.* 289, 30889-30899. <https://doi.org/10.1074/jbc.M114.604892>
- Rubio, P.S., Godoy, M.S., Della Mónica, I.F., Pettinari, M.J., Godeas, A.M., Scervino, J.M., 2015. Carbon and nitrogen sources influence tricalcium phosphate solubilization and extracellular phosphatase activity by *Talaromyces flavus*. *Curr. Microbiol.* 72, 41-47. <https://doi.org/10.1007/s00284-015-0914-7>
- Saepuloh, U., Iskandriati, D., Pamungkas, J., Solihin, D.D., Mariya, S.S., Sajuthi, D., 2020. Construction of a preliminary three-dimensional structure simian betaretrovirus serotype-2 (SRV-2) reverse transcriptase isolated from Indonesian cynomolgus monkey. *Trop. Life. Sci. Res.* 31, 47-61. <https://doi.org/10.21315/tlsr2020.31.3.4>
- Sakurai, M., Wasaki, J., Tomizawa, Y., Shinano, T., Osaki, M., 2008. Analysis of bacterial communities on alkaline phosphatase genes in soil supplied with organic matter. *Soil. Sci. Plant. Nutr.* 54, 62-71. <https://doi.org/10.1111/j.1747-0765.2007.00210.x>
- Sari, M., Nawangsih, A.A., Wahyudi, A.T., 2021. Rhizosphere *Streptomyces* formulas as the biological control agent of phytopathogenic fungi *Fusarium oxysporum* and plant growth promoter of soybean. *Biodiversitas.* 22, 3015-3023. <https://doi.org/10.13057/biodiv/d220602>
- Sati, S.C., Pant, P., 2019. Evaluation of phosphate solubilization by root endophytic aquatic hyphomycete *Tetracladium setigerum*. *Symbiosis.* 77, 141-145. <https://doi.org/10.1007/s13199-018-0575-y>
- Sharma, U., Pal, D., Prasad, R., 2014. Alkaline phosphatase: an overview. *Ind. J. Clin. Biochem.* 29, 269-278. DOI:10.1007/s12291-013-0408-y
- Shen, Y.C., Hu, Y.N., Shaw, G.C., 2016. Expressions of alkaline phosphatase genes during phosphate starvation are under positive influences of multiple cell wall hydrolase genes in *Bacillus subtilis*. *J. Gen. Appl. Microbiol.* 62, 106-109. <https://doi.org/10.2323/jgam.62.106>
- Soumare, A., Boubekri, K., Lyamlouli, K., Hafidi, M., Ouhdouch, Y., Kouisni, L., 2020. From isolation of phosphate solubilizing microbes to their formulation and use as biofertilizers: status and needs. *Front. bioeng. biotechnol.* 7, 425. <https://doi.org/10.3389/fbioe.2019.00425>
- Wahyudi, A.T., Priyanto, J.A., Fijrina, H.N., Mariastuti, H.D., Nawangsih, A.A., 2019. *Streptomyces* spp. from rhizosphere soil of maize with potential as plant growth promoter. *Biodiversitas.* 20, 2547-2553. <https://doi.org/10.13057/biodiv/d200916>
- Wahyudi, A.T., Fithriansyah, N.G., Amri, M.F., Priyanto, J.A., Nawangsih, A.A., 2021. Screening of chitinase-producing rhizosphere actinomycetes and their genetic diversity. *Biodiversitas.* 22, 4186-4192. <https://doi.org/10.13057/biodiv/d221008>
- Wan, W., Wang, Y., Tan, J., Qin, Y., Zuo, W., Wu, H., He, H., He, D., 2020. Alkaline phosphatase-harboring bacterial community and multiple enzyme activity contribute to phosphorus transformation during vegetable waste and chicken manure composting. *Bioresour. Technol.* 297, 122406. <https://doi.org/10.1016/j.biortech.2019.122406>
- Wong, C.K., Zulperi, D., Saidi, N.B., Vadmalai, G., 2021. A consortium of *Pseudomonas aeruginosa* and *Trichoderma harzianum* for improving growth and induced biochemical changes in *Fusarium wilt* infected bananas. *Trop. Life. Sci. Res.* 32, 23-45. <https://doi.org/10.21315/tlsr2021.32.1.2>
- Yang, J., Zhang, Y., 2015. Protein structure and function prediction using I-TASSER. *Curr. Protoc. Bioinform.* 52, 5-8. <https://doi.org/10.1002/0471250953.bi0508s52>
- Zhang, Y., 2008. I-TASSER server for protein 3D structure prediction. *BMC Bioinform.* 9, 40. <https://doi.org/10.1186/1471-2105-9-40>
- Zhu, X., Zhao, X., Lin, Q., Li, G., 2021. Distribution characteristics of *phoD*-harbouring bacterial community structure and its roles in phosphorus transformation in steppe soils in northern China. *J. Soil. Sci. Plant. Nutr.* 21, 1531-1541. <https://doi.org/10.1007/s42729-021-00459-3>